International Symposium on Rarefied Gas Dynamics, 23., Jul. 2002

300

Angle of Attack Effect on Rarefied Hypersonic Flow over Power Law Shaped Leading Edges

Wilson F. N. Santos* and Mark J. Lewis†

*Combustion and Propulsion Laboratory, INPE, Cachoeira Paulista, SP 12630-000, Brazil
†Department of Aerospace Engineering, University of Maryland, College Park, MD 20742, USA

Abstract. This paper deals with a numerical study of the aerodynamic surface quantities on power law shaped leading edges situated in a rarefied hypersonic flow. The sensitivity of the heat flux to, and pressure gradient on the body surface due to changes in the angle of attack is investigated by using a Direct Simulation Monte Carlo method. A method that has demonstrated to yield excellent comparisons with fight- and ground-test data, and that properly accounts for nonequilibrium aspects of the flow that arise near the nose of the leading edges. The work is motivated by the Newtonian flow theory that predicts that certain classes of power-law leading edges behave as aerodynamically sharp bodies at zero incidence, even though they are geometrically blunt. Calculations show that the pressure gradient follows that predicted by the Newtonian theory for the flow conditions considered.

INTRODUCTION

The successful design of high-lift, low-drag hypersonic configurations will depend on the ability to incorporate relatively sharp leading edges that combine good aerodynamic properties with acceptable heating rates. Certain configurations, such as hypersonic waveriders, are designed analytically with infinitely sharp leading edges for shock wave attachment. However, very sharp leading edges are not practical for a number of reasons: (1) very sharp leading edges are difficult to manufacture, (2) some blunting is required for structural strength, and (3) the heat transfer to sharp leading edges at high Mach numbers is severe.

The use of blunt-nose shapes tends to alleviate the aerodynamic heating problem since the heat transfer for blunt bodies is far lower than that for sharply pointed bodies. In addition, the reduction in heating rate for a blunt body is accompanied by an increase in heat capacity, due to the increased volume. Due mainly to manufacturing problems and the extremely high temperatures attained in hypersonic flight, hypersonic vehicles will have blunt nose, although probably slendering out at a short distance from the nose. Therefore, designing a hypersonic vehicle leading edge involves a tradeoff between making the leading edge sharp enough to obtain acceptable aerodynamic and propulsion efficiency and blunt enough to reduce the aerodynamic heating in the stagnation point.

Power law shaped leading edges ($y \propto x^n$, $0 < n < 1$) may provide the required bluntness for heat transfer, manufacturing and handling concerns with reduced departures from ideal aerodynamic performance. This concept is based on the work of Mason and Lee [1], who have pointed out that, for certain exponents, power law shapes exhibit aerodynamic properties similar to geometrically sharp shapes. They suggested the possibility of a difference between shapes that are geometrically sharp and shapes that behave aerodynamically as if they were sharp. Mason and Lee [1] showed that for values of $0 < n < 1/2$, the leading-edge radius of curvature goes to infinite at the nose, a characteristic of a blunt shape. For values of $1/2 < n < 1$ the leading-edge radius of curvature approaches zero at the nose, a characteristic of a sharp shape. Furthermore, for $2/3 < n < 1$, their computational investigation predicts that the derivative of the pressure coefficient with respect to the body coordinate dC_p/ds approaches $-\infty$ at $x = 0$, a characteristic of a sharp body. In this way, there is a class of body shapes given by $1/2 < n < 2/3$, for which the leading edge may behave aerodynamically like a blunt body, even though the leading-edge radius of curvature is zero, and another one given by $2/3 < n < 1$ for which the leading edge may behave like aerodynamically sharp body even though the leading edge bluntness is infinite. Their analysis describes the details of the geometry and aerodynamics of low-drag axisymmetric bodies by using Newtonian theory. However, one of the important aspects of the problem, stagnation point heat transfer, was not considered.

The sensitivity of both the pressure gradient and the stagnation point heating to shape variations of such leading edges was investigated by Santos and Lewis [2] for the idealized situation of two-dimensional rarefied hypersonic flow at zero angle of incidence. Through the use of Direct Simulation Monte Carlo (DSMC) method, they showed that the pressure gradient on the power law shapes in a rarefied environment is in surprising agreement with that obtained by Mason and Lee [1] by employing Newtonian analysis. It was found that the pressure gradient along the body surface goes to zero at the nose of the leading edge for $n < 2/3$, a characteristics of blunt body. It is finite for $n = 2/3$ and goes to minus infinite for $n > 2/3$, a characteristic of sharp body. Santos and Lewis [2] also found that the stagnation point heating behavior for power law leading edges with finite radius of curvature ($n = 1/2$), followed that predicted for classical blunt body, i.e., the heating rate on blunt bodies scales inversely with the square root of stagnation point radius. For those power law leading edges with zero radii of curvature ($n > 1/2$), the stagnation point heating is not a function of the curvature radius in the vicinity of the leading edges, but agrees with the classical blunt body behavior predicted by the continuum far from the stagnation point.

The purpose of this work is to investigate the impact of the angle of attack on the behavior of the pressure gradient and the stagnation point heating. For positive angle of attack, important changes occur in the flowfield structure and in the aerodynamic surface quantities on blunt leading edges. This involves the modification of the flowfield properties and shock strength and, consequently, some effects on aerodynamic forces acting on, and on heat transfer to the body surface. Moreover, the knowledge of these properties at zero angle of attack is not sufficient to predict with certainty the flow characteristics over these shapes with incidence. In this context, the essential characteristics of the angle of attack effect on both pressure gradient and stagnation point heating will be examined for power law bodies defined by exponents of 1/2, 2/3 and 3/4, and positive angle of attack with 5, 8 and 12 degree of incidence. In the current study, DSMC method will be employed to calculate the rarefied hypersonic two-dimensional flow.

LEADING EDGE GEOMETRY DEFINITION

The power-law shapes, $y = ax^n$, are modeled by assuming a sharp leading edge of half angle θ with a circular cylinder of radius R inscribed tangent to this wedge. The power law shapes, inscribed between the wedge and the cylinder, are also tangent to the wedge and the cylinder at the same common point where they have the same slope angle. It was assumed that the leading edge half angle is 10°, a circular cylinder diameter of 10^{-2}m and power law exponents of 1/2, 2/3, and 3/4. Figure 1 illustrates schematically this construction for this set of power law leading edges.

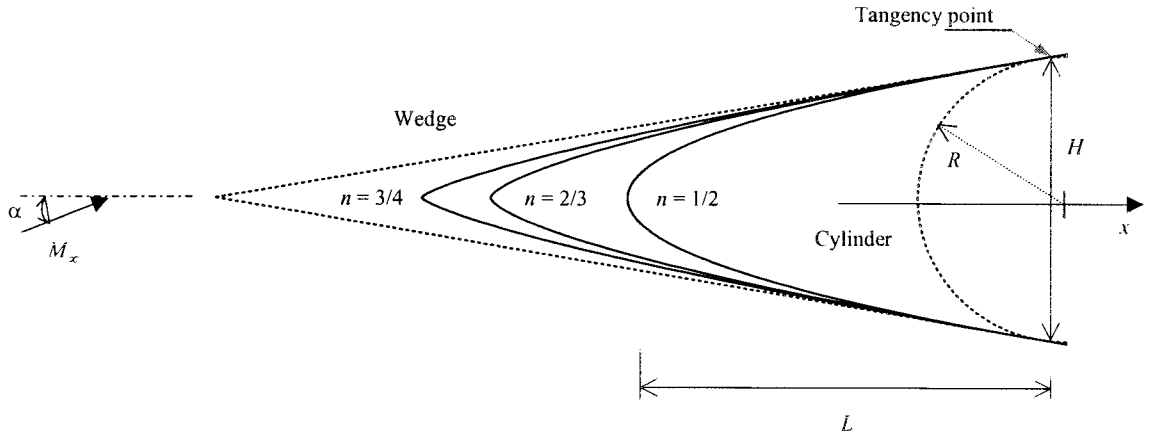

FIGURE 1. Drawing illustrating the leading edge geometry.

From geometric considerations, the power law constant a is obtained by matching slope on the wedge, circular cylinder and power law body at the tangency point. The common body height H at the tangency point is equal to $2R\cos\theta$, and the body length L from the nose to the tangency point in the axis of symmetry is given by $nH/2\tan\theta$.

COMPUTATIONAL METHOD AND PROCEDURE

A number of significant problems in fluid mechanics involve flows in the transitional regime, i.e., flows for which the Knudsen number is larger than 0.01 and less than 10. The most successful numerical technique for modeling complex flows in the transitional regime has been the Direct Simulation Monte Carlo (DSMC) method [3].

DSMC models the flow as being a collection of discrete particles, each one with a position, velocity and internal energy. The state of the particles is stored and modified with time as the particles move, collide, and undergo boundary interactions in simulated physical space. The physical space is represented by a computational cell network. The cell provides a convenient reference for the choice of the potential collision pairs and for the sampling of the macroscopic gas properties. The dimensions of the cells must be such that the change in flow properties across each cell is small. The linear dimensions of the cells should be small in comparison with the scale length of the macroscopic flow gradients in the streamwise directions, which means that the cell dimensions should be of the order of the local mean free path or even smaller [3]. The smallest unit of physical space is the subcell, where the collision partners are selected for the establishment of the collision rate. In addition, the time step ought to be sufficiently small in comparison with the local mean collision time [3].

In this study, the molecular collisions are modeled using the variable hard sphere (VHS) molecular model [4]. This model employs the simple hard sphere angular scattering law so that all directions are equally possible for post-collision velocity in the center-of-mass frame of reference. However, the collision cross section depends on the relative speed of colliding molecules. The energy exchange between kinetic and internal modes is controlled by the Borgnakke-Larsen statistical model [5]. The essential feature of this model is that a fraction of the collisions is treated as completely inelastic, and the remainder of the molecular collisions is regarded as elastic. Simulations are performed using a nonreacting gas model consisting of two chemical species, N_2 and O_2. Energy exchanges between the translational and internal modes are considered. The vibrational temperature is controlled by the distribution of energy between the translational and rotational modes after an inelastic collision. The probability of an inelastic collision determines the rate at which energy is transferred between the translational and internal modes after an inelastic collision. For a given collision, the probabilities are designated by the inverse of the relaxation numbers, which correspond to the number of collisions necessary, on average, for a molecule to relax. For this study, the relaxation numbers of 5 and 50 were used for the rotation and vibration, respectively. The effective number of degrees of freedom in the partially excited vibrational states is calculated from the harmonic oscillator theory.

The freestream and flow conditions used in the present calculations are those given by Santos and Lewis [2] and summarized in Table 1. The freestream velocity U_∞ is assumed to be constant at 3.5 Km/s, which corresponds to freestream Mach number M_∞ of 12. The wall temperature T_w is assumed constant at 880 K. Also, diffuse reflection with full thermal accommodation is assumed for the gas-surface interactions. The overall Knudsen number, defined as the ratio of the molecular mean free path in the freestream gas to the diameter of the circular cylinder, corresponds to $Kn_\infty = 0.0903$. Finally, the freestream Reynolds number by unit length Re_∞ is 21455.

The computational domain used for the calculations, the grid generation scheme, the effect of grid resolution and the complete validation process employed in this study are described in details in Ref. [6].

TABLE 1. Freestream Conditions and Flow Parameters.

Altitude		70	Km
Temperature (T_∞)		220.0	K
Pressure (p_∞)		5.582	N/m^2
Density (ρ_∞)		8.753×10^{-5}	Kg/m^3
Number density (n_∞)		1.8209×10^{21}	m^{-3}
Viscosity (μ_∞)		1.455×10^{-5}	Ns/m^2
Velocity (U_∞)		3.56	Km/s
Mean free path (λ_∞)		9.03×10^{-4}	m
Molecular weight		28.96	Kg/KgMole
Mole fraction	O_2	0.237	
Mole fraction	N_2	0.763	
Molecular mass	O_2	5.312×10^{-26}	Kg
Molecular mass	N_2	4.65×10^{-26}	Kg
Molecular diameter	O_2	4.01×10^{-10}	m
Molecular diameter	N_2	4.11×10^{-10}	m

COMPUTATIONAL RESULTS AND DISCUSSION

The impact of the angle of attack on the pressure acting on and the heat transfer to the body surface resulting from DSMC simulations are highlighted in this section.

The pressure p_w on the body surface is calculated by the sum of the normal momentum fluxes of both incident and reflected molecules at each time step. A flux is regarded as positive if it is directed toward the surface. Results are normalized by the freestream dynamic pressure $\frac{1}{2}\rho_\infty U_\infty^2$ and presented in terms of the pressure coefficient C_p.

The dependence of the pressure coefficient due to variations in the angle of attack is demonstrated in Figures 2, 3 and 4 for power law exponents of 1/2, 2/3 and 3/4, respectively. In this set of Figures, the plots in the left side represent the pressure coefficients along the windward sides of the leading edges, while the plots in the right side those in the leeward sides. Also, the dimensionless arc length is measured from the stagnation point along the body surface for the case of zero degree of incidence. For purpose of comparison, the pressure coefficients for these power law shapes by considering zero degree angle of attack [2] are also presented in this set of Figures.

According to these Figures, by increasing the incidence causes the expected asymmetry in the pressure coefficient as the stagnation point moves from the axis to the lower windward side. The pressure coefficient presents the expected behavior in that it increases in the windward side and decreases in the leeward side with increasing the angle of attack.

Referring to Figure 2, the maximum values for the pressure coefficient in the windward side, which correspond to angles of attack of 5, 8 and 12 degrees are located at stations $-s/\lambda_\infty = 0.06$, 0.17 and 0.19, respectively. The locations of the stations which are identified with the points of tangency of the normal to the flow direction and the body surface are $-s/\lambda_x = 0.08$, 0.14 and 0.21 for 5, 8 and 12 degrees of incidence, respectively. Consequently, the geometric stagnation point does not correspond to the aerodynamic stagnation point. For the other power law cases, the same behavior is observed, however, it takes place closer to the axis of symmetry.

Newtonian flow [1] predicts that the derivative of pressure coefficient with respect to body coordinate dC_p/ds approaches $-\infty$ at $x = 0$ for axisymmetric power law shapes in the range $2/3 < n < 1$. However, Newtonian flow assumes an infinite Mach number, ratio of specific heats equal to one, and a shock shape that matches the body shape.

In order to compare the validity of the Newtonian approximations in predicting the pressure gradient behavior, dC_p/ds was estimated for the $n = 3/4$ case from the DSMC solutions. The qualitative behavior of the pressure gradient is depicted in Figure 5, parameterized by the angle of attack α. For purpose of comparison, the pressure gradient for the case of zero degree of incidence is also illustrated in this Figure. According to this Figure, the pressure gradient presents the expected behavior in that it approaches $-\infty$ as the arc length goes to zero. In this way, the pressure gradient behaves as if the leading edge were a blunt one in spite of the fact that the leading edge has a zero radius of curvature.

The heat flux q_w to the body surface is calculated by the net energy fluxes of the molecules impinging on the surface. The net heat flux is related to the sum of the translational, rotational and vibrational energies of both incident and reflected molecules. The heat flux is normalized by $\frac{1}{2}\rho_\infty U_\infty^3$ and presented in terms of heat transfer coefficient C_h.

The impact on heat transfer coefficient due to changes in the angle of attack is illustrated in Figures 6, 7 and 8 for power law exponents of 1/2, 2/3 and 3/4, respectively. According to this set of Figures, the heat transfer coefficient follows the same trend observed for pressure coefficient in that it increases in the windward side and decreases in the leeward side with increasing the incidence. The heat transfer coefficient presents the maximum value in the stagnation region and drops off a short distance away of the leading edge nose as the power law exponent increases. Also, it is seen that the blunter the leading edge the lower the heat transfer coefficient in the vicinity of the stagnation point.

A number of theoretical and numerical predictions of stagnation point heat transfer on blunt bodies have been reported in the literature [7-13]. Theoretical formulations, experimental data, and semi-empirical formulas all agree in the fact that stagnation point heat transfer for blunt bodies is inversely proportional to the square root of the nose radius ($q_w \propto 1/\sqrt{R_n}$). In this context, it seems to be interesting to investigate this behavior for the power law shaped leading edges, that are blunt by definition ($dy/dx \to \infty$ at $x = 0$), even though the radius of curvature at the nose goes to zero for $n > 1/2$.

In order to verify the dependence of the heat transfer coefficient C_h on the leading edge radius of curvature, the product $C_h \sqrt{(R_c/\lambda_x)}$, named here by function $K(n,\alpha)$, was obtained from the DSMC results. Figures 9 and 10 display the function $K(n,\alpha)$ along the body surface for power law exponents of 1/2 and 3/4, respectively. These Figures also show the function $K(n,\alpha)$ for the case of zero angle of attack [2].

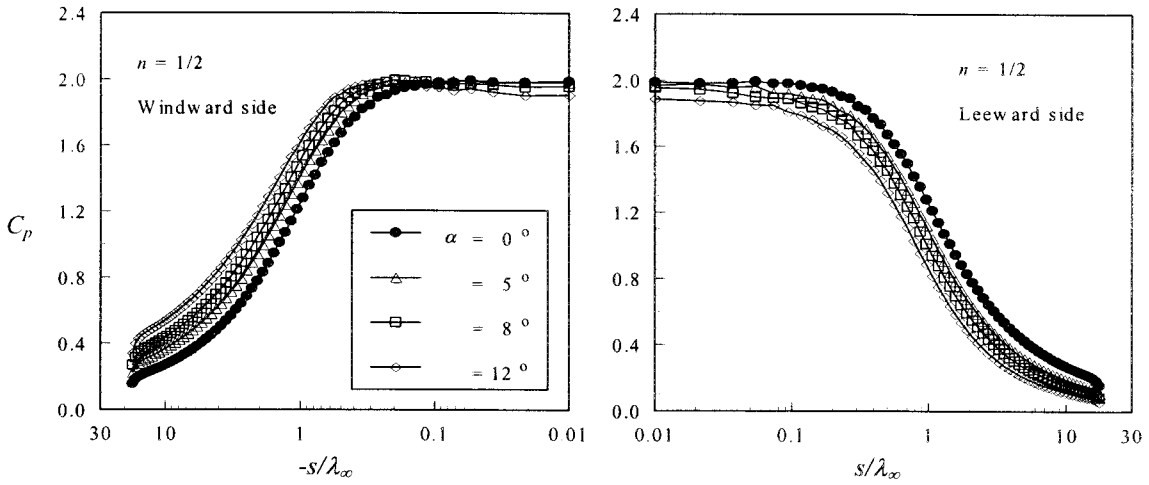

FIGURE 2. Effect of the angle of attack on pressure coefficient along the windward side (left) and leeward side (right) of body surface for power law exponent of 1/2.

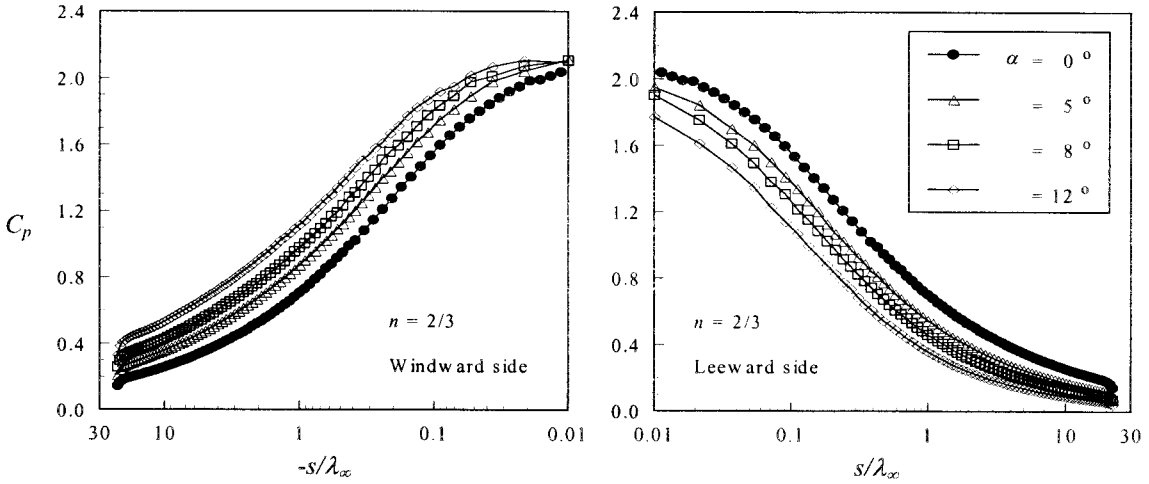

FIGURE 3. Effect of the angle of attack on pressure coefficient along the windward side (left) and leeward side (right) of body surface for power law exponent of 2/3.

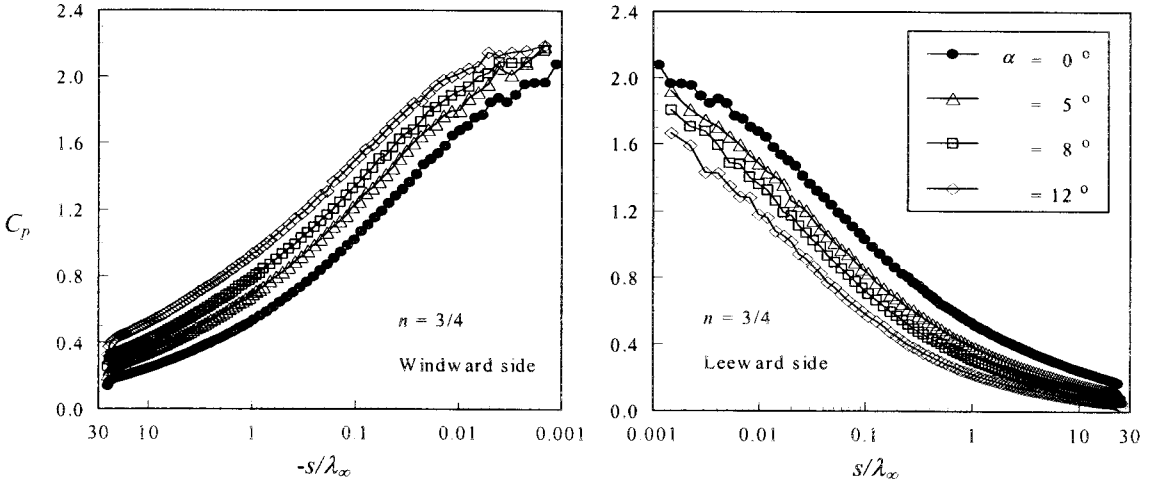

FIGURE 4. Effect of the angle of attack on pressure coefficient along the windward side (left) and leeward side (right) of body surface for power law exponent of 3/4.

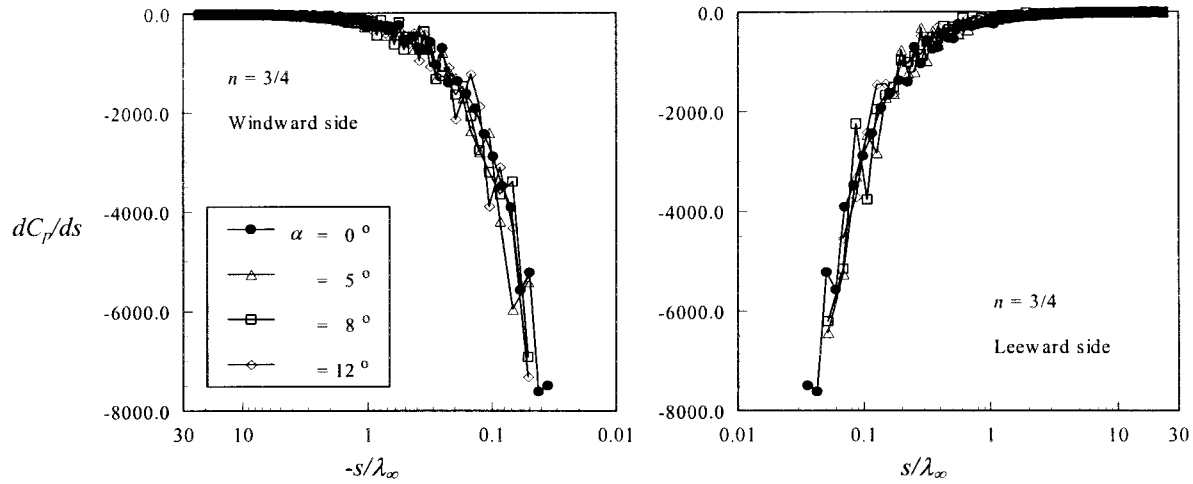

FIGURE 5. Pressure gradient behavior along the windward side (left) and leeward side (right) of body surface for power law exponent of 3/4.

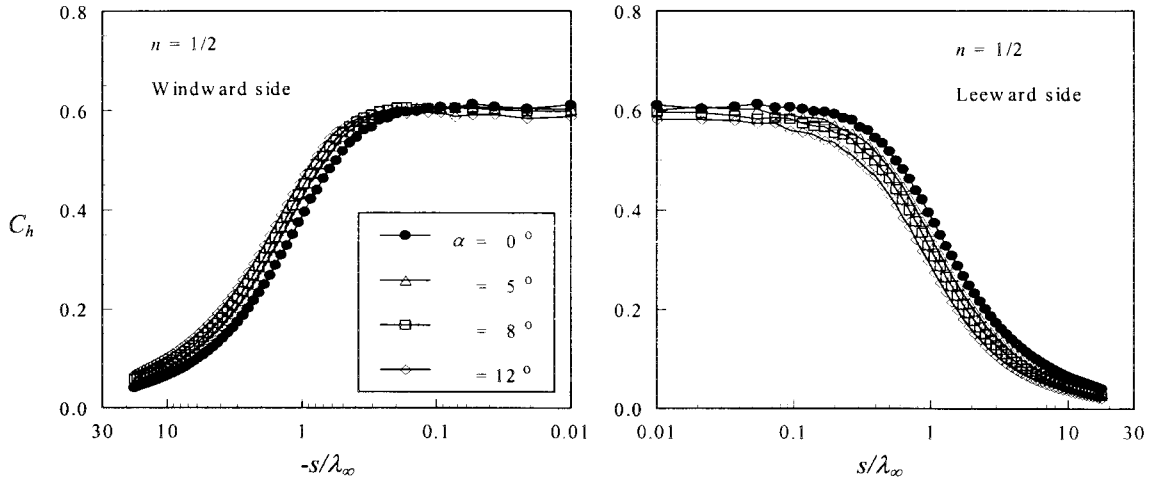

FIGURE 6. Effect of the angle of attack on heat transfer coefficient along the windward side (left) and leeward side (right) of body surface for power law exponent of 3/4.

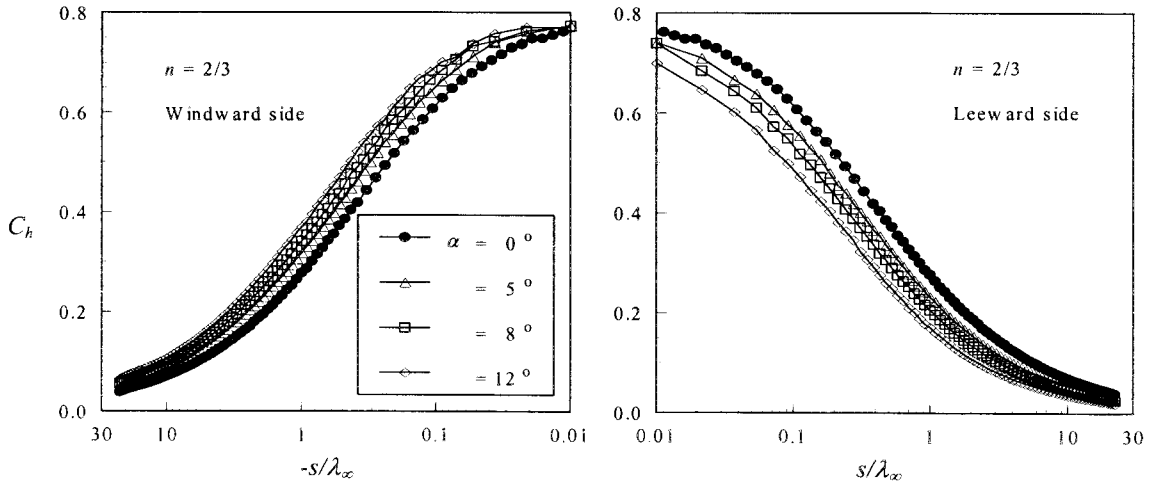

FIGURE 7. Effect of the angle of attack on heat transfer coefficient along the windward side (left) and leeward side (right) of body surface for power law exponent of 3/4.

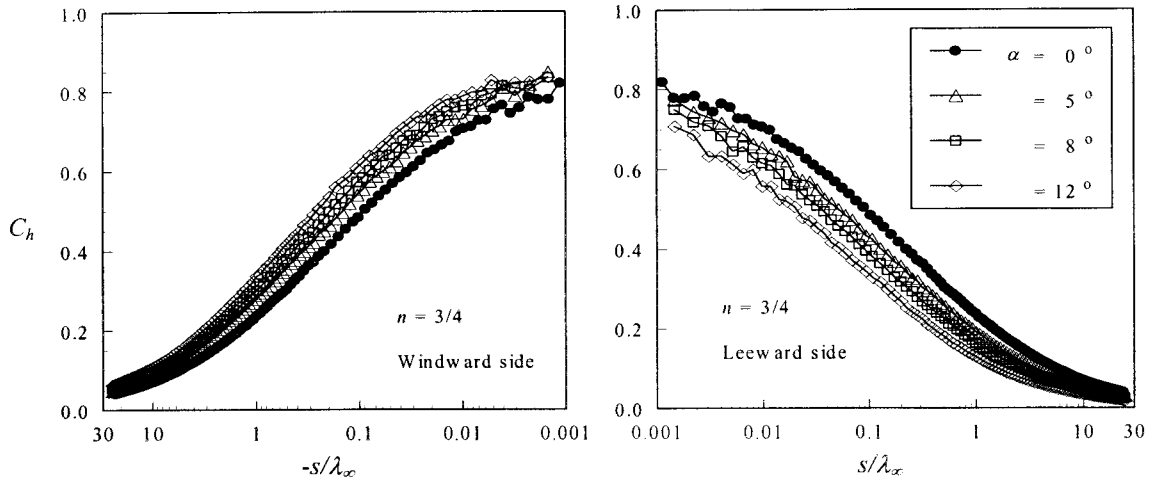

FIGURE 8. Effect of the angle of attack on heat transfer coefficient along the windward side (left) and leeward side (right) of body surface for power law exponent of 3/4.

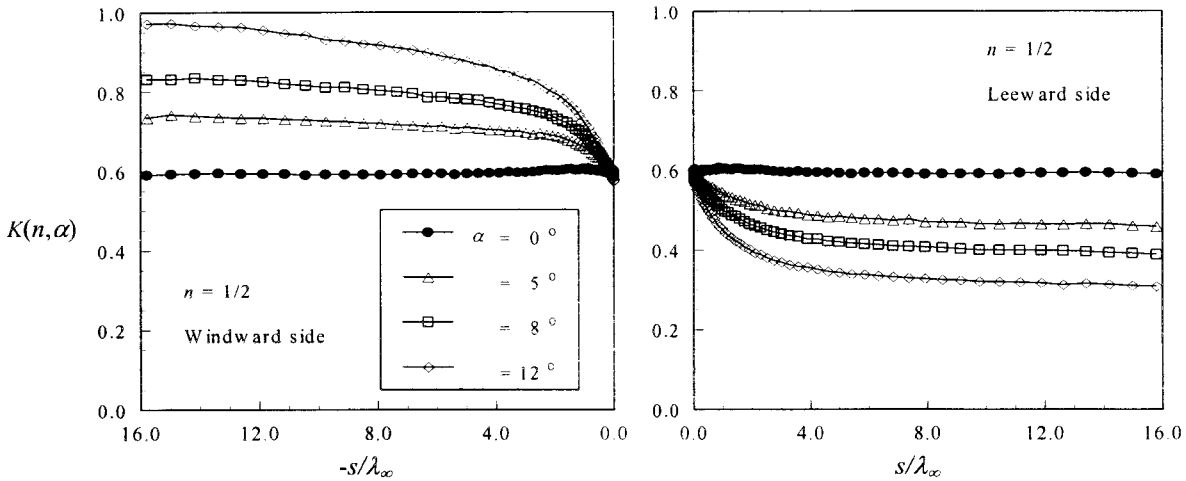

FIGURE 9. Effect of the angle of attack on the product $C_h\sqrt{(R_c/\lambda_\infty)} \equiv K(n,\alpha)$ along the windward side (left) and leeward side (right) of body surface for power law exponent of 1/2.

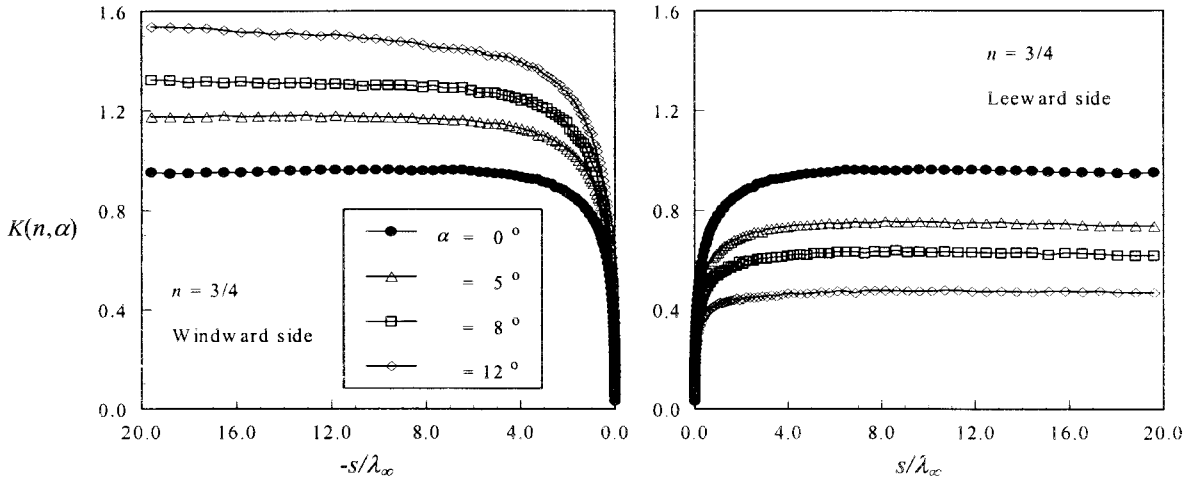

FIGURE 10. Effect of the angle of attack on the product $C_h\sqrt{(R_c/\lambda_\infty)} \equiv K(n,\alpha)$ along the windward side (left) and leeward side (right) of body surface for power law exponent of 3/4.

Interesting features can be drawn from Figures 9 and 10. In the vicinity of the stagnation point, the dependence of the heat transfer coefficient on the radius of curvature follows that predicted by the continuum flow for power law shapes with finite radius, $n = 1/2$ case, and zero angle of attack. Furthermore, it fails for the $n > 1/2$ cases for which the radii of curvature approach zero at $x = 0$. Moreover, the function $K(n,\alpha)$ tends to a constant value downstream the stagnation region for the range of incidence investigated. The constant value, which is a function of the power law exponent and angle of attack, is reached faster in the leeward side than that in the windward side.

CONCLUDING REMARKS

This study applies the Direct Simulation Monte Carlo method to assess the angle of attack effect on aerodynamic surface quantities of power law shaped leading edges. The calculations provided information concerning the nature of the pressure coefficient and heat transfer coefficient at the vicinity of the nose resulting from variations in the leading edge thickness at incidence for the idealized situation of two-dimensional hypersonic rarefied flow at 70 km of altitude. Performance results for 5, 8 and 12 degrees of incidence for power law exponents of 1/2, 2/3 and 3/4 were compared to those cases for zero degree angle of attack.

The simulations confirmed the qualitative behavior of the pressure coefficient predicted by the Newtonian theory. It was found that, even though at incidence, the pressure gradient along the both windward and leeward sides of the power law leading edges goes to minus infinite for $n > 2/3$ cases. Thus, leading edges with $n > 2/3$ produce a flowfield that does not exhibit classical blunt body behavior, and can be considered as if they were sharp for the calculation of pressure distribution.

Another issue that stimulated this study was the heat transfer rate. It was also found that the heat flux to power law shaped leading edges follows that for classical blunt body far from the nose of the leading edges in that it scales inversely with the radius of curvature. This dependence with the radius of curvature is more significant in the leeward side than that in the windward side with increasing the angle of attack, and it disappears in the vicinity of the stagnation point.

ACKNOWLEDGMENTS

The first author is grateful to the High Performance Computer Center (NACAD-COPPE/UFRJ) at the Federal University of Rio de Janeiro and the Weather Prediction Center and Climate Studies (CPTEC/INPE) at the National Institute for Space Research for use of the workstations.

REFERENCES

1. Mason, H. W., and Lee, J., *Journal of Spacecraft and Rockets* **31(3)**, 378-382, (1994).
2. Santos, W. F. N., and Lewis, M. J., "Power Law Shaped Leading Edges in Rarefied Hypersonic Flow," *in 40th AIAA Aerospace Sciences Meeting and Exhibit*, AIAA paper 2002-0645, Reno, NV, 14-17 January 2002.
3. Bird, G. A., *Molecular Gas Dynamics and the Direct Simulation of Gas Flows*, Oxford University Press, Oxford, England, UK, 1994.
4. Bird, G. A., "Monte Carlo Simulation in an Engineering Context," *in Progress in Astronautics and Aeronautics: Rarefied gas Dynamics*, edited by Sam S. Fisher, Vol. 74, part I, AIAA, New York, 1988, pp. 239-255.
5. Borgnakke, C. and Larsen, P. S., *Journal of computational Physics* **18**, 405-420, (1975).
6. Santos, W. F. N., "Direct Simulation Monte Carlo of Rarefied Hypersonic Flow on Power Law Shaped Leading Edges," Ph.D. Dissertation, Dept. of Aerospace Engineering, University of Maryland, College Park, MD, Dec., 2001.
7. Sibulkin, M., *Journal of Aeronautical Sciences* **19(8)**, 570-571, (1952).
8. Lees, L., *Jet Propulsion* **26(4)**, 259-269, (1956).
9. Romig, M., *Jet Propulsion* **26(12)**, 1098-1101, (1956).
10. Fay, J. A., and Riddell, F. R., *Journal of Aeronautical Sciences* **25(2)**, 73-85, (1958)
11. Zoby, E., Moss, N. J. and Sutton, K., *Journal of Spacecraft and Rockets* **18(1)**, 64-70, (1981).
12. DeJarnette, F. R., Hamilton, H. H., Weilmuenster, K. J., and Cheatwood, F. M., *Journal of Thermophysics and Heat Transfer* **1(1)**, 5-12, (1987).
13. Zuppardi, G., and Verde, G., *Journal of Spacecraft and Rockets* **35(3)**, 403-405, (1998).